Multimethod characterization of a chlorinated solvents contaminated site and geoelectrical monitoring of in-situ bioremediation

Nivorlis, Aristeidis

2020

Document Version:
Publisher's PDF, also known as Version of record

Multimethod characterization of a chlorinated solvents contaminated site and geoelectrical monitoring of in-situ bioremediation

ARISTEIDIS NIVORLIS
ENGINEERING GEOLOGY | FACULTY OF ENGINEERING | LUND UNIVERSITY

Printed by Media-Tryck, Lund 2020 NORDIC SWAN ECOLABEL 3041 0903

Division of Engineering Geology
Faculty of Engineering
Lund University
ISBN 978-91-7895-622-7
ISRN LUTVDG/(TVDG-1044)/(1-97)/(2020)

Multimethod characterization of a chlorinated solvents contaminated site and geoelectrical monitoring of in-situ bioremediation

Licentiate Thesis

Aristeidis Nivorlis
Division of Engineering Geology
Lund University
Sweden

2020-08-27

LUND
UNIVERSITY

Faculty of Engineering, Engineering Geology

ISBN (print) 978-91-7895-622-7
ISBN (pdf) 978-91-7895-623-4
ISRN LUTVDG/(TVTG-1044)/(1-97)/(2020)

Printed in Sweden by Media-Tryck, Lund University
Lund 2020

Abstract

Soil contamination is a widespread problem and actions need to be taken in order to prevent damage to the groundwater and the life around the contaminated sites. In Sweden more than 80.000 sites are potentially contaminated, therefore there is a demand for accurate and efficient methods for site characterization and soil remediation. In the past, the preferred methodology for soil remediation involved the excavation of the contaminated mass which was either deposited in landfills (dig and dump) or treated elsewhere (dig and treat). However, these techniques are associated with significant high risk (secondary exposure) and long-term costs. On the other hand, in-situ bioremediation has the potential to address these issues offering a safer, more sustainable and cost-efficient alternative for soil remediation. Unfortunately, monitoring the progress of in-situ treatments requires soil/water sampling and laboratory analysis, which, if done frequently, can increase the cost dramatically. For this reason, there is a demand for new methodologies that can be used to follow the progress of in-situ bioremediation.

The work presented in this thesis involves a former dry-cleaning facility located in Alingsås (Sweden). The site is contaminated with chlorinated solvents and a pilot in-situ bioremediation plan was launched in November 2017. First, we adapted a multimethod approach for site characterization using several methods: Direct Current resistivity and time-domain Induced Polarization (DCIP), Seismic Refraction Tomography (SRT) and the Membrane Interface Probe (MIP). The aim was to build a refined geological conceptual model. Second, we developed an autonomous and fully automated system for geophysical monitoring with the DCIP method that aims to follow the daily changes in the subsurface. We present a complete workflow that includes data acquisition, pre-processing, inversion and visualization of the daily DCIP monitoring data. The proposed scheme is robust and shows that DCIP monitoring has great potential to record the changes due to the bioremediation; however, it needs to be paired with more information (temperature, geochemistry, contaminant concentrations) to better understand the changes that take place in the subsurface.

Sammanfattning

Förorenad mark är ett utbrett problem och åtgärder måste vidtas för att förhindra skador på grundvattnet och ekosystem runt de förorenade platserna. I Sverige är mer än 80 000 områden förorenade, därför krävs det tillförlitliga och effektiva metoder för platsundersökning och marksanering. Den traditionellt använda metoden för marksanering består av utgrävning av den förorenade massan med påföljande deponering (gräva och deponera) eller behandling någon annanstans (gräva och ex-situ behandla). Dessa tekniker är dock förknippade med betydande risk (sekundär exponering) och kostnader. In-situ sanering genom biologisk nedbrytning har potential att erbjuda ett säkrare, mer hållbart och kostnadseffektivt alternativ för marksanering. Detta kräver dock kontroll av resultatet genom övervakning av effekten av åtgärderna via provtagning och laboratorieanalys, vilket, om det görs ofta, kan öka kostnaderna dramatiskt och endast bidrar med punktformig data. Av denna anledning finns det behov av nya metoder som kan användas för att följa och verifiera effekterna av den initierade biologiska nedbrytningen på plats.

Det arbete som presenteras i denna avhandling omfattar ett pilotförsök för sanering vid en tidigare kemtvättanläggning belägen i Alingsås (Sverige). Platsen är förorenad med klorerade lösningsmedel och pilotförsöket med in-situ sanering initierades i november 2017. Vi utarbetade undersökningar och övervakning med hjälp av flera olika metoder: kombinerad elektrisk resistivitetstomografi och tidsdomän Inducerad Polarisation (DCIP), seismisk refraktionstomografi (SRT) och membraninterfaceprob (MIP). Syftet var att bygga en förfinad geologisk konceptuell modell för att förstå marksystemet. Vidare utvecklade vi ett autonomt och helautomatiserat system för geofysisk övervakning med DCIP-metoden som syftar till att dagligen följa förändringarna i marken. Vi presenterar ett komplett arbetsflöde som inkluderar datainsamling, databehandling, inversion och visualisering av de dagliga DCIP-mätningarna. Det föreslagna arbetsflödet är robust och visar att DCIP-övervakning har stor potential att registrera kemiska förändringarna till följd av biologisk sanering; emellertid måste den kopplas ihop med mer information (t.ex. temperatur, geokemi, koncentration av föroreningar) för att bättre förstå de förändringar som sker i marken.

Preface

The work of this thesis has been carried out at the Division of Engineering Geology, Lund University in Sweden.

I want to thank my main supervisor Torleif Dahlin and my assisting supervisor Matteo Rossi for excellent support, help and guidance throughout my work. I would also like to thank my assisting supervisors Gianluca Fiandaca, Panagiotis Tsourlos and Alfredo Mendoza for providing valuable comments on my work. Furthermore, I would like to thank my colleagues within the MIRACHL group for their fruitful discussions and suggestions during the planning of the fieldwork and the analysis of the results and my colleagues at the Division of Engineering Geology for a friendly and supportive working environment. Finally, I would like to thank my family for their love and support.

This work has been carried out within the MIRACHL project (http://mirachl.com/). Funding is provided by the Swedish Research Council Formas—The Swedish Research Council for Environment, Agricultural Sciences and Spatial Planning (ref. 2016-20099), SBUF—The Development Fund of the Swedish Construction Industry (ref. 13336), ÅForsk (ref. 14-332), SGU—Swedish Geological Survey, Sven Tyréns stiftelse, Västra Götalandsregionen and Lund University.

Aristeidis Nivorlis

Lund, August 2020

List of appended papers

The following two papers are appended in the thesis. The thesis author has contributed to the design of the monitoring system, conducted the major part of the fieldwork required to ensure that the installations are functioning correctly and programmed the automation of measurements and data streaming. The thesis author has performed major parts of the data analysis and interpretation for the appended articles. As the main author, he has been the leading writer of the appended articles, with support and input on specific parts from the co-authors. The co-authors have contributed to the design and installation of the monitoring system, and to the interpretation of the results.

Paper I

Nivorlis, A.; Dahlin, T.; Rossi, M.; Höglund, N.; Sparrenbom, C. Multidisciplinary Characterization of Chlorinated Solvents Contamination and In-Situ Remediation with the Use of the Direct Current Resistivity and Time-Domain Induced Polarization Tomography.

Geosciences 2019, 9, 487.

Paper II

Nivorlis, A.; Dahlin, T.; Rossi, M. Temporal filtering and time-lapse inversion of geoelectrical data for monitoring of in-situ bioremediation

Submitted for publication (Geophysical Journal International)

Table of Contents

Chapter 1. Introduction

Soil contamination is a widespread problem that has been recognized in the past decades as the governments and global organizations move towards sustainability and green development. The directive of environmental liability (2004/35/CE) established a common framework based on the 'polluter pays' principle among the countries that are members of the European Union. On that basis, more than 80.000 potentially contaminated sites (SEPA, 2014) have been identified by the Swedish Environmental Protection Agency (SEPA). Therefore, there is a demand for modern methodologies for site characterization and soil remediation that are more effective, more efficient, minimize the risk for secondary exposure and are potentially cheaper to deploy on a large scale.

In this context, in-situ bioremediation is an attractive alternative to traditional remediation techniques, such as 'dig and dump', 'dig and treat' or 'thermal remediation', especially in cases where the contaminants have migrated deep into the subsurface, are spread over a large area or are located in urban environments and specifically underneath buildings. However, one draw-back of in-situ bioremediation is that there are no efficient methodologies to monitor the changes that take place in the subsurface and to estimate the effectiveness of the treatment. Currently, the most common way to monitor the remediation is done through periodical water samples from pre-installed wells that will only reflect the dissolved contaminants in water, usually a small fraction of the total pollution. Furthermore, it requires qualified staff to interact directly with the contaminant and should be kept to the minimum. Geophysical methods can provide a useful tool to extrapolate the time-step point information acquired from drilling and water sampling to further increase our understanding about the subsurface and the changes that take place during a remediation experiment.

The Electrical Resistivity Tomography (ERT) has been successfully used in a wide range of subsurface investigations (Loke et al., 2013) such as hydrogeological (Chirindja et al., 2017; Fetter, 2001; Giang et al., 2018; Leroux and Dahlin, 2006; Zago et al., 2020), environment (Auken et al., 2014; Fernandez et al., 2019; Forquet and French, 2012), engineering geology (Abdulsamad et al., 2019; Danielsen and Dahlin, 2009; Rossi et al., 2018) and archaeological (Angelis et al., 2018; Argote-Espino et al., 2016; Simyrdanis et al., 2018a). The Direct Current resistivity and time-domain Induced Polarization tomography (DCIP) is an extension to the traditional ERT survey and measures an additional property, the chargeability,

whilst recent developments (Olsson et al., 2016, 2015) make it possible to record the two electrical properties simultaneously and more efficiently. The DCIP has been successfully used to solve more complex problems such as lithology mapping (Kemna et al., 2004; Slater and Lesmes, 2002), landfill characterization (Bernstone et al., 2000; Chambers et al., 2006; Gazoty et al., 2012b; Ntarlagiannis et al., 2016; Power et al., 2018; Ustra et al., 2012; Wemegah et al., 2017) and microbial activity (Atekwana et al., 2005; Atekwana and Atekwana, 2010; Davis and Atekwana, 2006; Slater et al., 2008). Frequency based spectral Induced Polarization has been applied to monitoring of stimulated bioremediation of uranium contamination with promising results (Flores Orozco et al., 2013), while DCIP has been used to monitor groundwater contamination and leakage (Kuras et al., 2016; Leroux et al., 2010; Park et al., 2016) and gas migration within landfills (Rosqvist et al., 2011; Steelman et al., 2017). In sites contaminated with Non-Aqueous Phase Liquids (NAPLs), DCIP has been successfully applied for characterization (Johansson et al., 2017; Maurya et al., 2018; Power et al., 2014; Simyrdanis et al., 2018b) and monitoring of the changes due to remediation (Caterina et al., 2017; Sparrenbom et al., 2017). The successful use of frequency domain IP for monitoring of free-phase hydrocarbon contamination (Cassiani et al., 2009) injection and transport of microscale zerovalent iron (mZVI) particles for groundwater remediation purposes (Flores Orozco et al., 2015) introduce more opportunities for the DCIP method to be used in that field.

Previous work with geophysical monitoring involves several DCIP measurements which are recorded in consecutive time steps. There are systems that can automatically record more frequent measurements(Chambers et al., 2009), the data are usually processed manually and the results include selected time-steps even though several recordings are available. Therefore, it is of paramount importance to develop and propose efficient and robust routines to be able to deploy scalable geophysical systems that autonomously and automatically collect data without running into the problem of being overloaded with manual processing.

Aim, objectives and limitations

The overall aim of this study is to follow the changes of an in-situ bioremediation experiment with the use of geophysics and namely the DCIP method.

The first objective is to use the information from geophysical methods (DCIP and Seismic Refraction Tomography) and the information from the Membrane Interface Probe method (lithology and contaminant concentration) to improve the geological conceptual model for the contaminated site. The second objective is to develop efficient and robust routines for quality control, pre-processing, inversion, and visualization of the daily DCIP monitoring data.

DCIP provides a detailed description of the subsurface, in both space and time and has great potential when used to extrapolate the time-step point information from traditional sampling techniques The resulting DCIP monitoring models need to be further calibrated and jointly interpreted with water and soil sampling. The proposed scheme for processing and inversion is developed based on the data from the Alingsås site. It is suggested that this scheme is tested and potentially calibrated before applied to another site.

Outline

The outline of this Licentiate thesis is as follows: chapter 2 describes the area of investigation where chapter 3 gives a background description of the methods used in this thesis with emphasis on the geoelectrical method DCIP. Chapter 4 presents the geoelectrical monitoring and the challenges that are associated with it. The main results are summarized in chapter 5 and the conclusions as well as an overview of the future work are presented in chapter 6.

Chapter 2. Site description

In Alingsås (South Central Sweden, see Figure 1), an industrial-scale dry-cleaning facility (Alingsåstvätteriet) started operating in 1963, supplying cleaning services for the military. Sometime during the 1960s or 1970s, a single spill of approximately 200 L of PCE leaked into the ground, resulting in the formation of a DNAPL source zone beneath the building with a plume extending out under the parking lot. That is the only documented spill; however, other instances of undocumented spills could have occurred in the past. Today, the use of PCE has ceased, and the facility is operating under the Administrative Region Västra Götaland as a laundry and textile cleaning (water only) unit, taking care of approximately 40 tons of textiles per day for the regional hospitals. Responsibility for the remediation is shared between the Swedish Government, through the Swedish Geological Survey (SGU) and the current owners (Region Västra Götaland). Due to ongoing operations in the building, in-situ remediation is the favored approach for treatment of the contaminated mass.

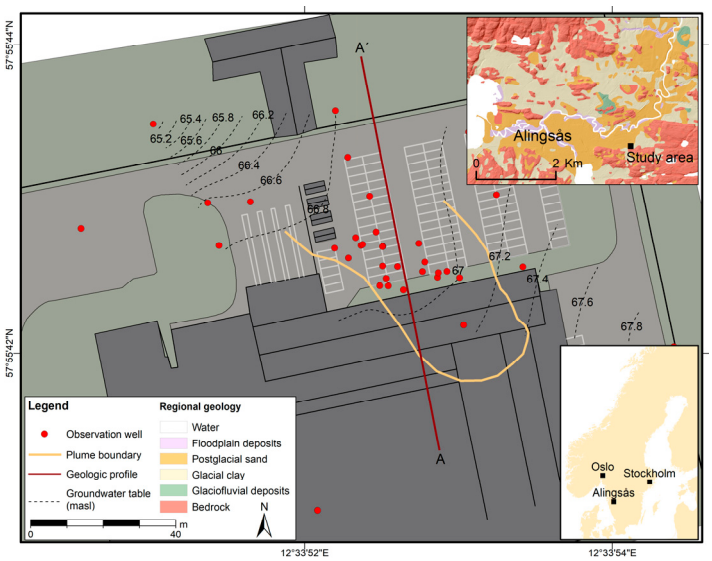

Figure 1. Overview of the Alingsås site where the observation wells (red circles), the groundwater level (black dashed lines), the plume boundaries (orange line) and the regional surface geology (top right, created with data from SGU Jordarter, 1:25,000–1:100,000 © SGU) can be seen. Line A-A' marks the location of geological conceptual model shown in Figure 2.

In the area of investigation, the depth to the crystalline bedrock varies between 2 to 12 m. The sediment overlying the bedrock is deposited in a fining upwards sequence. It consists of a unit of sand with lenses of silt and clay, followed by a layer of clay and on top of the sediment, about 1 m of fill material is present. The geological conceptual model, modified from Branzen (2013), is presented in Figure 2. The sedimentary units show a varying inner heterogeneity with lenses of both finer and coarser material occurring. The bedrock topography slopes gently towards N. The depth to the water table varies between 1.5 to 2 m below the ground surface and the groundwater flows from SE towards NW as can be seen in Figure 1.

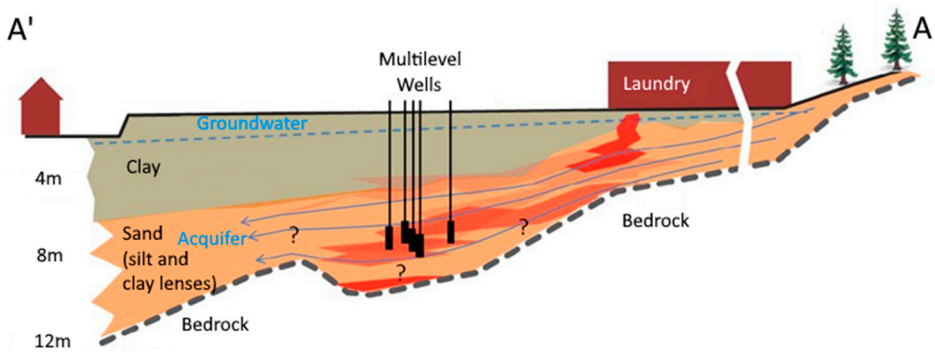

Figure 2. Geological conceptual model (S-N). (Modified from Branzen, 2013).

In order to determine the best approach for treatment of the contamination and to stop further spreading, a pilot in-situ remediation program was launched in November 2017, using a direct push injection method on the north side of the laundry building (Figure 3). In order to evaluate the best approach for a future full-scale remediation scenario, two different remediating agents were injected into the plume at different locations, for comparison. In injection area A (west side, see Figure 3) Provectus ERD-CH4™ substrate containing a carbon source (electron donor) in the form of vegetable oils together with acids and a bacterial consortium (Dehalococcoides mccartyi, Desulfovibrio, Desulfitobacterium and methanogenic archaea bacteria) was injected in two phases between the 7th and the 17th of November 2017, at a total of 32 points. In injection area B (east side, see Figure 3) CAT100™ substrate containing granular activated carbon, zero-valent iron and Trap & Treat® bacteria concentrate were injected, together with a methane inhibitor, between the 28th and the 30th of November 2017, at a total of 37 points. In both cases, the products were injected from a depth of 3 m and downward until reaching the top of the bedrock.

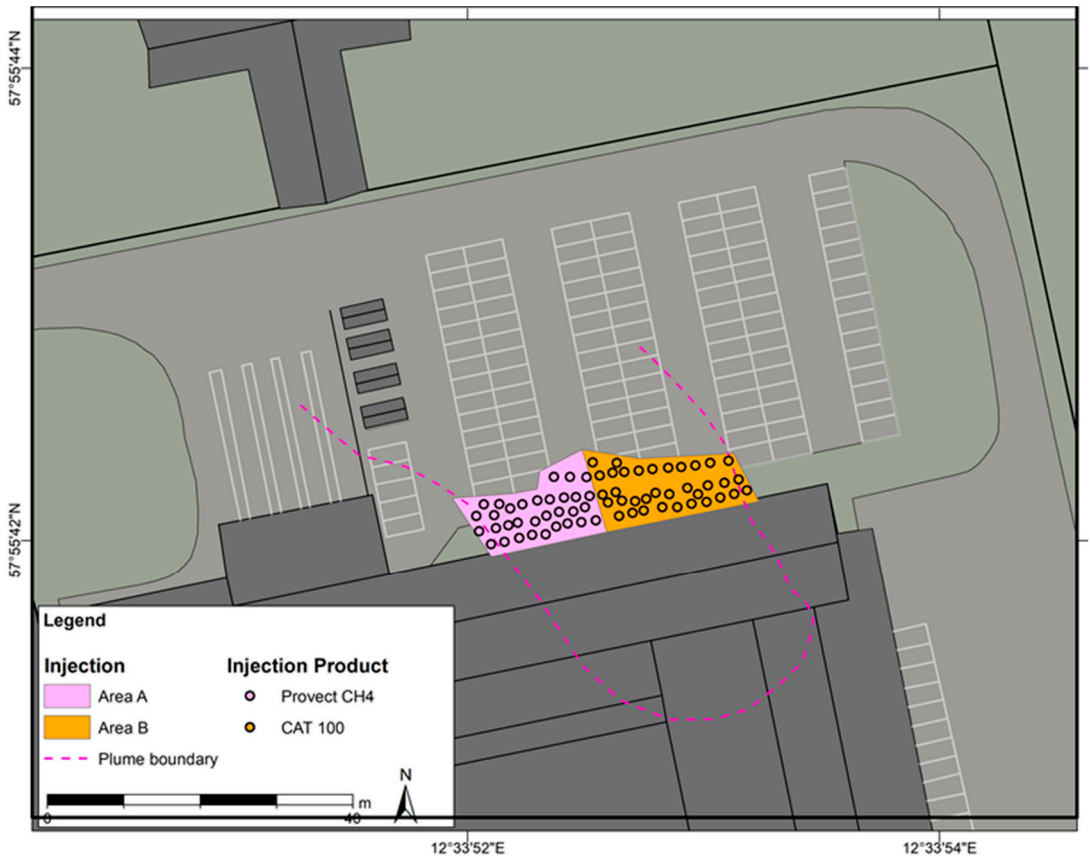

Figure 3. Pilot in-situ bioremediation plan launched during November 2017.

Chapter 3. Methods

The Direct Current resistivity and time-domain Induced Polarization tomography (DCIP) method was primarily used in this thesis work, therefore this method will be described in some detail. The SRT, MIP and temperature monitoring methods used as complementary methods to the DCIP will be introduced briefly to obtain a clear overview of the overall methodology used in this work.

Direct Current resistivity and time-domain IP

The Direct Current resistivity and time-domain Induced Polarization (DCIP) method includes the use of the traditional resistivity method and its extension, the induced polarization method. The former measures the distribution of the electrical resistivity where the latter measures the capacity of the ground to store charges. Recent advances in the past years, both in terms of hardware and software, made it possible to measure both quantities simultaneously making the acquisition faster and more accurate therefore increasing the popularity of the method significantly. The essential theory of the DCIP method, which is required to follow the thesis work, is described in this chapter.

Resistivity method

The electrical resistivity, ρ ($\Omega \cdot m$) is a fundamental property that quantifies the opposition of a material, the ground in our case, to the flow of electrical currents. For a single resistivity measurement four electrodes are employed, two electrodes are used to inject the current (A and B) and two, usually different, electrodes (M and N) are used to measure the potential difference (Figure 4).

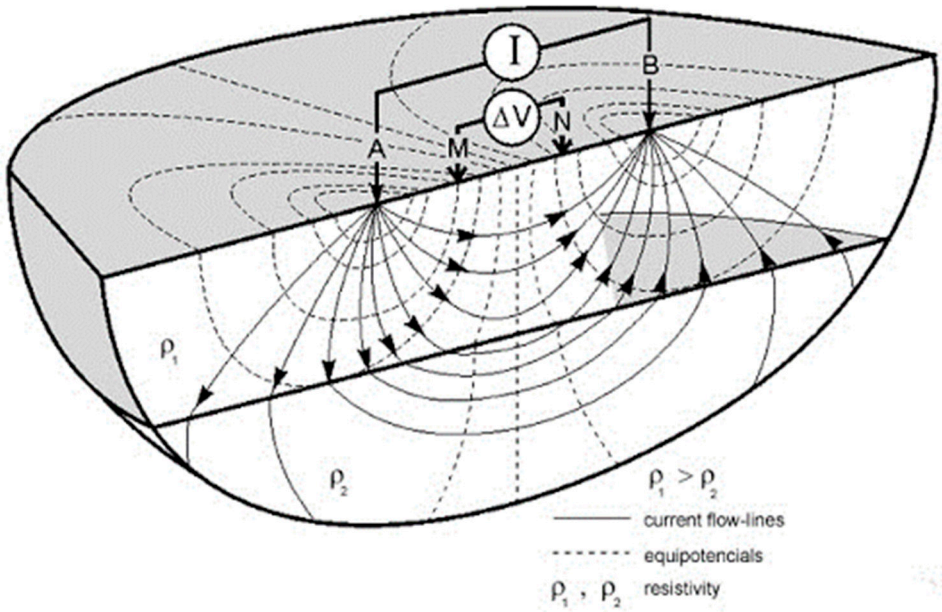

Figure 4. Single resistivity measurement. (Original figure provided by Knödel et al., 2007).

The Ohmic resistance (R) of the ground is calculated using the formula:

$$R = \frac{V}{I} \tag{1}$$

where V is the potential difference and I is the electrical current injected into the ground. By taking the position of the four electrodes into account, the electrical resistivity can be calculated using the formula:

$$\rho = R\frac{2\pi}{G} \tag{2}$$

where the geometric factor G can be calculated using the formula:

$$G = \frac{1}{AM} - \frac{1}{BM} - \frac{1}{AN} + \frac{1}{BN} \tag{3}$$

The electrical resistivity calculated from equation *(2)* corresponds the true electrical resistivity only in cases of a homogeneous and isotropic media. However, the earth is, in most cases, heterogeneous so the previous calculations do not generally yield the true electrical resistivity of the ground. The electrical resistivity calculated by the equation *(2)* represents a kind of weighted average, although this is not mathematically correct (Cook and Van Nostrand, 1954), of the resistivities of the different subsurface materials and is called the apparent resistivity.

Induced Polarization

The induced polarization method can be considered as an extension of the resistivity method, as a similar configuration as described in Figure 4 is required. In addition to the electrical resistivity calculation another parameter called apparent chargeability is measured. This parameter measures the ability of the ground to store current in form of electrical energy during the injection of the current, acting very similarly to a capacitor.

In order to measure the energy stored, after each current injection (on time) there is an intermediate pause step where no current is injected (off time). During the off time instead of the voltage being zero, because no current is applied, the stored electrical energy is released and is recorded by the instrument as a gradual drop in the voltage before it drops down to zero (Figure 5).

The apparent chargeability as defined by Siegel (1959) is the ratio between the secondary voltage immediately after the current is turned off (Vs) and the primary voltage, while the current is on (Vm), as can be seen in Figure 5 left. In reality, the secondary voltage cannot be accurately measured because when the current turns off electromagnetic effects are produced. These electromagnetic effects can be several orders of magnitude higher than the secondary voltage and this makes it very difficult to separate the two signals. For this reason, modern instruments record the chargeability by integrating over the voltage curve several milliseconds after the current is turned off (Figure 5 right and equation (*4*)).

$$m = \frac{1}{V_m}\int_{t_1}^{t_2} V_s(t)\,dt = \frac{\sum_{i=1}^{n}(M_i TM_i)}{\sum_{i=1}^{n} TM_i} \qquad (4)$$

Where V(t) is the function of voltage over time, V_m is the voltage before the current cut off, M_i is the integral chargeability and T_i is the time window of the i_{th} gate.

It is obvious that the chargeability is a dimensionless parameter which cannot be larger than 1 because the secondary voltage will always be lower than the primary.

It is possible to encounter negative apparent chargeability values that can be explained in view of negative sensitivity areas (Dahlin and Loke, 2015). This means that the apparent chargeability can range from -1 to 1 V/V or -1000 to 1000 mV/V. The latter form (mV/V) is more commonly encountered.

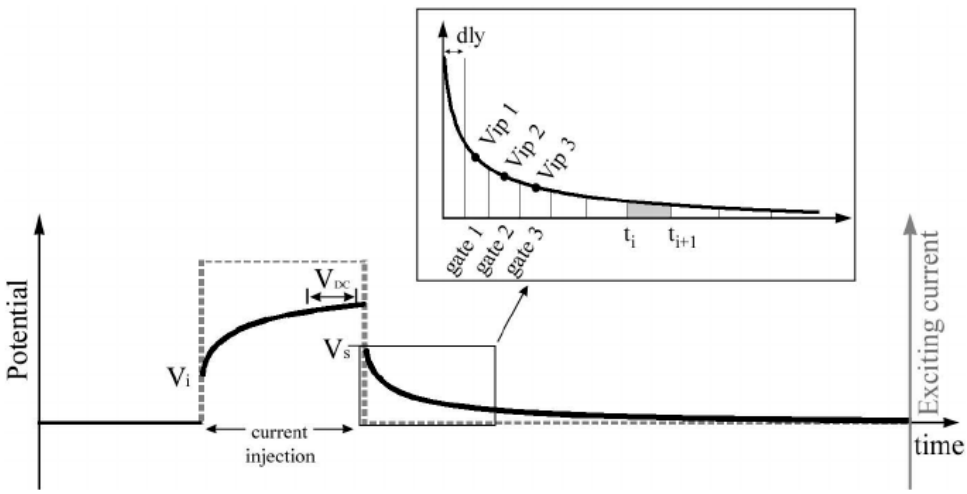

Figure 5. Chargeability as defined by Siegel (main plot) and as measured by modern instruments (small plott) (Gazoty et al., 2012a).

Electrical Resistivity Tomography

The principles described in the previous sections, describes a single measurement, using four (4) electrodes or a quadrupole, which gives very limited information about the subsurface due to the presence of heterogeneities. For that reason, in a DCIP survey we perform hundreds of single measurements using several combinations of electrodes that are preplaced and connected to the instrument. The instrument performs a series of single measurement with 4 electrodes, based on a given predefined sequence, until all the desired 4-electrode combinations are measured. This type of survey is often called Electrical Resistivity Tomography (ERT) and can be further explained in Figure 6. The total number of possible combinations could be thousands, however several specific configurations, called electrode arrays, are more frequently used. In this thesis work we have mainly used the multiple gradient array (Dahlin and Zhou, 2006) which has high signal to noise (S/N) ratio making it particularly suitable for IP measurements.

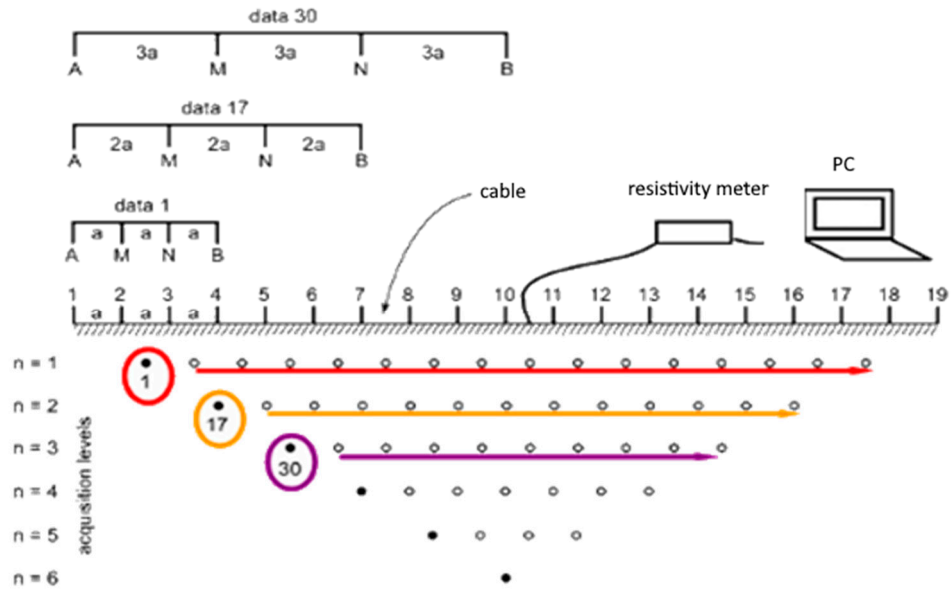

Figure 6. DCIP field survey (modified after Loke and Barker, 1996).

As discussed previously, during a DCIP survey current is injected into the ground and the potential difference is recorded between several receiver pairs. For the 2D case, several arrays offer advantages and within this thesis work the multiple-gradient array (Dahlin and Zhou, 2006) was used. The observations (apparent resistivities) can be plotted in a pseudo-section and illustrate a distorted representation of the distribution (Figure 7) of the electrical properties in the ground.

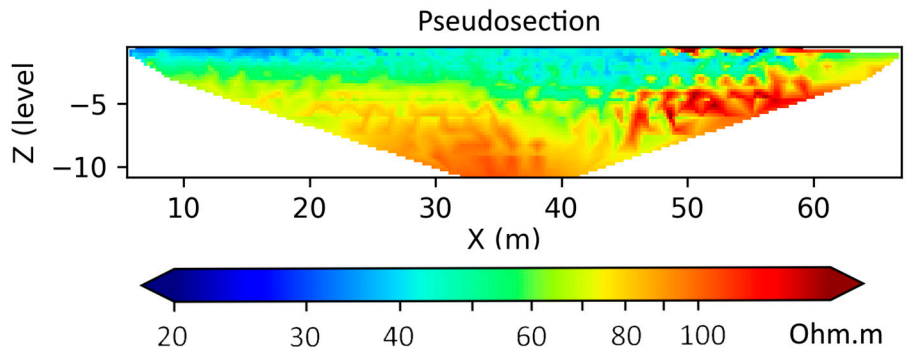

Figure 7. Pseudosection that represents the distribution of apparent resistivities in the ground (observations).

Forward Modelling

The forward modeling involves the calculation of the response of a model representing the earth's structure for which the electrical resistivity distribution is known. To solve this problem, for given source locations the current flow inside the model needs to be simulated. The equation that governs the current flow in the ground is the Poisson equation:

$$\nabla\,(-\sigma\nabla V) = \nabla J \tag{5}$$

Where V is the potential, σ represents the subsurface conductivity and J describes the current sources.

Although analytical solutions do exist for simple geometries (Cook and Van Nostrand, 1954) for more complex geometries they do not exist. For complex geometries, the eq. 5 is solved using a numerical approach such as the finite element method (FEM) which is used in this work (Loke et al., 2014, 2011). In FEM the earth is divided into a finite number of smaller homogeneous and isotropic cells, called elements. Each element is assigned a value of the electrical properties, as described extensively in (Tsourlos and Ogilvy, 1999) and the solution to eq.(*5*) is approximated.

Inversion

As previously described, it is rather straight forward to calculate the response of an array given a known distribution of the electrical properties. However, the distribution of the electrical properties is usually unknown and needs to be determined. That can be achieved through an iterative process called inversion, which tries to find the distribution of parameters that gives theoretical measurements that best fit the real data. The smoothness constrained inversion (Tsourlos and Ogilvy, 1999) is the algorithm that is used in this work to solve the inverse problem and is briefly described in Figure 8.

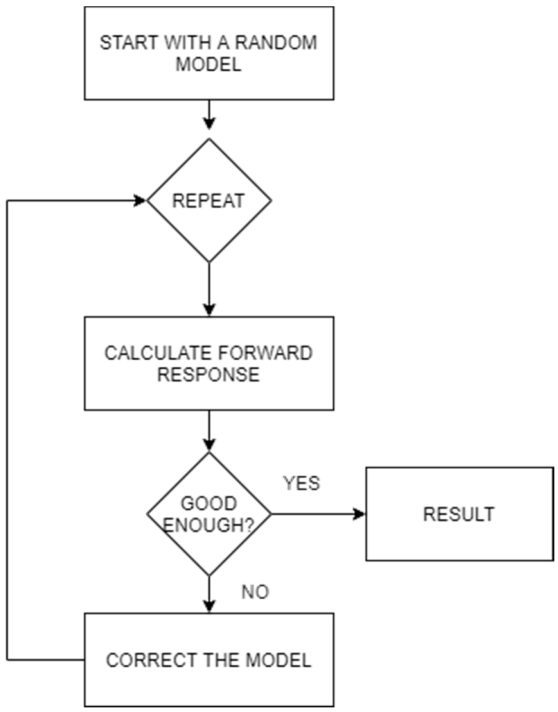

Figure 8. Simplified diagram that describes the general inversion algorithm.

To begin with, a homogeneous earth is most commonly used for the initial model. The model response is calculated (forward solution) then the model is compared with the observed measurements and the misfit is computed. If one of the stopping criteria is met the process terminates, otherwise the model is updated, and the process is repeated. The criteria for terminating the process that are commonly used include a maximum number of iterations, no further improvements in the solution or a solution with an acceptable misfit.

The observations are used by the inversion algorithm to find the distribution of parameters (resistivities) that will generate synthetic measurements (forward response) that are as close as possible.

The distribution of the electrical properties (inverted profile, Figure 9) can be linked with the lithology and with the presence of water or contaminants. The connection however is not trivial and a priori information about the area of investigation is required to interpret the results. Last, it is important to mention that the distribution of the electrical properties can vary through time because of seasonal variations, such as temperature changes and rainfall events, changes in groundwater level and geochemistry. The last is of great importance in this thesis work, because during the in-situ bioremediation the properties of the subsurface are changing, therefore one inverted profile captures a single time-step of the overall changes.

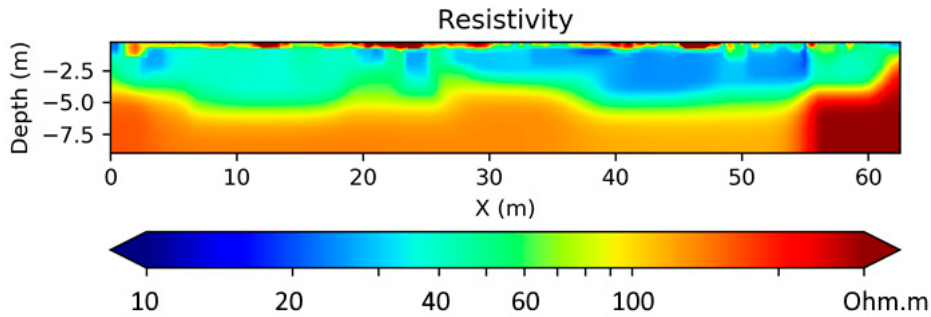

Figure 9. True distribution of resistivities (properties) in the subsurface.

Complementary Methods

Membrane Interface Probe

The Membrane Interface Probe (MIP) is a logging method where a probe, equipped with sensors, is directly pushed into the ground in a way similar to a cone penetration test (CPT). First and foremost, the probe is equipped with a detector that can measure the volatile hydrocarbon and solvent contamination at different depths. Moreover, other sensors attached to the probe can estimate the electrical conductivity and hydraulic permeability of the geological units at different depths.

The method is efficient for mapping the contaminants in-situ in the subsurface, while at the same time information that can be used to describe the lithology can be provided. However, the MIP method only provides time specific single point information about the subsurface and additional methods are needed to achieve more continuous spatial coverage.

Seismic Refraction Tomography

The seismic refraction method estimates the velocity with which a generated elastic wave propagates into the subsurface. A source such as a hammer, explosion or an accelerated weight drop is used to generate, in this case, compressional waves (P-waves), although shear waves (S-waves) could be used as well. The generated waves contain information about the media that they are propagated through and are recorded at several receivers, the geophones, placed at different distances from the

source. The experiment is repeated by moving the source to other positions, thus generating more waves, to obtain further information about the elastic properties of the subsurface (P wave velocity) that can be used to describe the lithology.

In the traditional seismic refraction method, the first arrivals are used to estimate the depth to the refractors, interfaces where the elastic properties (P-wave velocity) change. The groundwater table or the transition from one lithological unit to another are examples of refractors that can be identified by the seismic refraction method.

Seismic Refraction Tomography introduces a more advanced approach where instead of identifying refractors (surfaces) a model of the elastic properties of the subsurface (P-wave velocity) is estimated. That is achieved by an inversion approach, similar to the one described for the DCIP, where a system of non-linear equations are solved to generate a model of the P-wave velocities for the subsurface (White, 1989).

Temperature monitoring

The monitoring of the soil temperature is essential when deploying geoelectrical monitoring systems because the electrical properties are directly affected by the temperature. Even though the electrical properties are affected by temperature, it is not possible to delineate the temperature of the subsurface from the DCIP data, making it paramount to use external probes for that purpose.

The variations of the temperature can be used to understand the changes that take place in the subsurface and understand how the geoelectrical signal can potentially be affected. The effects of seasonal variations can be observed by monitoring the temperature of the soil at different depth intervals. Furthermore, rainfall events can also affect the temperature of the soil, apart from changing the water saturation, and therefore may be identified from the soil temperature data.

Chapter 4. DCIP Monitoring

DCIP monitoring

As mentioned previously, the electrical properties of the subsurface often change over time, for example due to variations in the soil temperature, water content or the contamination levels. In these scenarios DCIP measurement can be repeated several times, using exactly the same setup, to make it possible to record the changes in the electrical properties of the subsurface. Then, it becomes possible to produce several inverted profiles that represent the distribution of the electrical properties over time thus revealing how the subsurface is changing over time. This approach is called DCIP monitoring.

The DCIP monitoring is carried out by repeating the geophysical survey consecutive times and often requires several data acquisition campaigns in the area of investigation. The frequency that each individual measurement is recorded and the time-span of the monitoring survey depends on the overall scope. Frequent measurements are needed to capture and understand the more rapid changes, for example due to rainfall events, and longer survey experiments are required to make it possible to identify changes that are usually slower, such as remediation experiments. Furthermore, the seasonal variations (yearly) due to temperature are usually dominant in the shallow layers, introducing the challenge of identifying changes that relate to environmental (gas migration, leachates, contaminations etc.) or engineering geology (soil stabilization, internal erosion in dams) problems.

To address these problem, it is important to have a system that can acquire frequent data for long periods which would require the DCIP equipment (cables, electrodes and instrumentation) to be deployed in the field introducing several risks (damage to the equipment, public safety and theft). This can be solved by deploying a permanent installation (Figure 10), where the cables and the sensors are buried under the ground and the instrument is stored safely in a nearby building (if possible).

To achieve frequent measurements, for example daily, robust routines for data collection need to be developed to make it possible to automatically collect DCIP without the need of an on-site team. In addition, schemes for managing the collected data should be present, so that data are safely archived and backed up after the

collection. Lastly, tools for quality control of the entire procedure are important to be in-place and produce warnings in case of failure.

Figure 10. Permanent installation of electrodes for a DCIP monitoring experiment. Alingsås, Sweden.

Challenges in data processing

The daily collected data from a DCIP monitoring system are often affected by noise. Although it is not common, a system failure might occur therefore gaps in the data are also to be expected. Spatial noise in the data can be observed by analysing the pseudosections that are recorded daily (Figure 11) where temporal noise can be seen by isolating the observed values (apparent resistivities and chargeabilities) of individual quadrupoles (Figure 12) over the entire timespan of a monitoring system. Moreover, frequent daily measurements can quickly accumulate creating large datasets and manual processing is no longer an efficient option for data processing.

There is an inherent need for efficient and robust schemes for filtering large datasets, removing extreme outliers and potentially bad data points that do not appear to be coherent with their neighbouring values (space domain) or their past and future values (time domain).

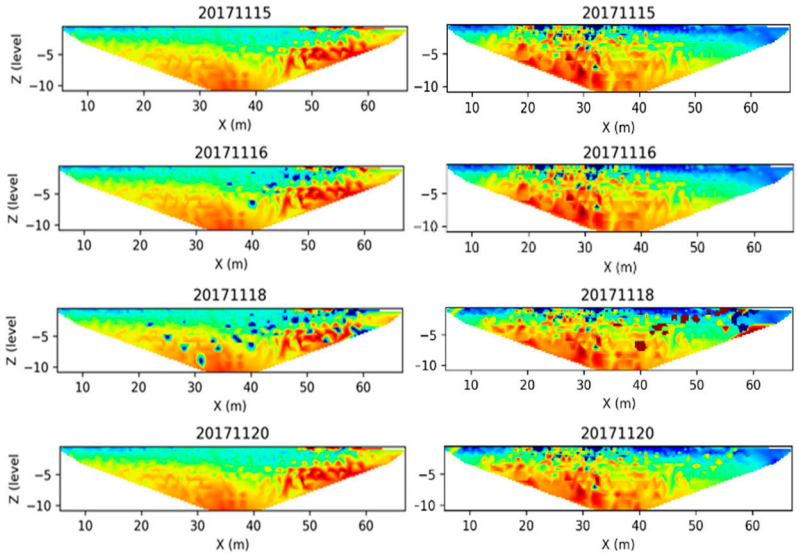

Figure 11. Spatial outliers in the observed apparent resistivity (left) and apparent chargeability (right)) data. Data from individual profiles presented as pseudosections.

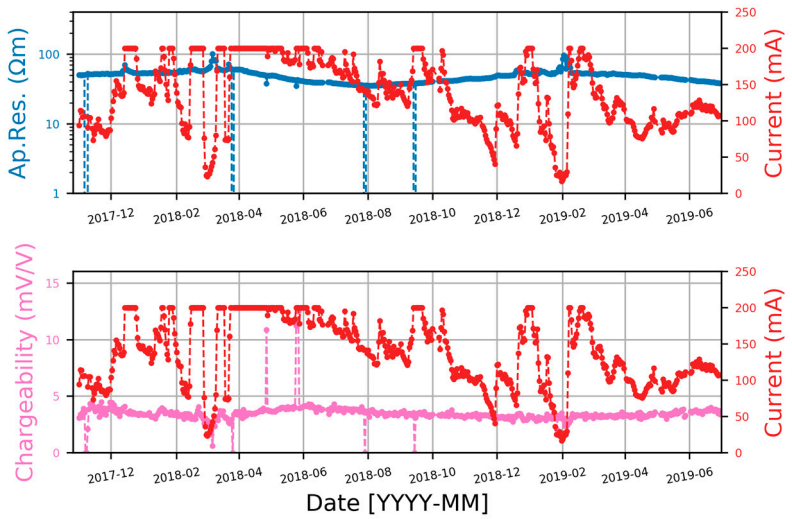

Figure 12. Temporal outliers in the observed apparent resistivity (top) and apparent chargeability (bottom)) data. Data from a single quadrupole presented as time-series.

Inversion results and visualization

The inversion of monitoring data is an active topic of research. The naïve approach of inverting individual datasets separately is not effective (Kim et al., 2013) as the resulting models could potentially introduce artificial changes (artefacts). Advanced algorithms and efficient routines are needed to estimate models that better describe the subsurface.

In this context, two algorithms are of significant importance and should be mentioned. The time-lapse inversion algorithm (Loke et al., 2014) introduces an additional time constraint in the traditional smoothness constrain inversion. The algorithm solves the inverse geoelectrical problem for two datasets simultaneously and estimates two models of the subsurface while preserving spatial continuity of the electrical properties between the models. The 4D inversion algorithm (Kim et al., 2013; Loke et al., 2014) further expands that idea by simultaneously estimating several geoelectrical models instead of two.

In the 4D algorithm the data space is increased exponentially therefore rapidly making inversions computationally expensive and making it inefficient to invert many datasets at once. Furthermore, in cases where a new dataset is recorded daily it might be inefficient to invert all the previous steps again, since the solution for the previous data are already computed. For that reason, an optimal solution needs to be identified that produces good quality results and which can be efficiently executed multiple times.

Chapter 5. Main Results

Paper I

Paper I adopts a multimethod approach for site characterization by using the MIP, SRT and DCIP method.

First, the MIP soundings were used to create the geological profiles (Figure 13) and describe the geology in the study area. The concentrations of the contaminants measured by the MIP soundings, show that the highest concentrations of contaminants are found in the clay layer. Also, the presence of a thin sandy layer above the bedrock acts as a porous media that flushes the contaminant downstream.

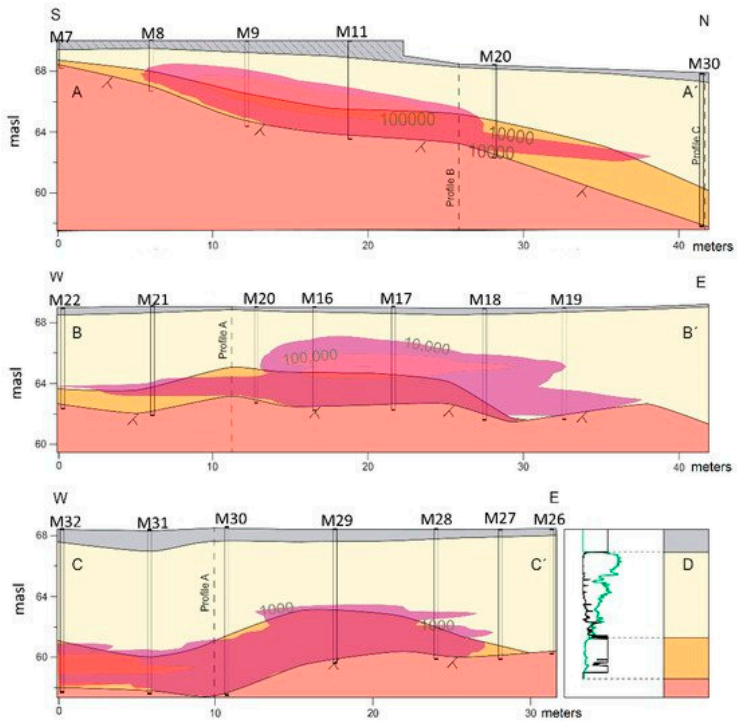

Figure 13. Geological profiles created from MIP data. Filling material (grey), fine material (yellow), coarse material (orange) and bedrock (red). The contamination is indicated by the purple contour map.

The contaminants sink into the sediments, since they are heavier than water, until they reach an impermeable layer, and then they can continue to migrate along its slope. In Alingsås, the crystalline bedrock is expected to act as an impermeable layer, although there are no drillings to verify that the contaminants haven't spread in there. For that reason, the SRT was used to estimate the bedrock topography for a larger area covering the parking lot. The bedrock topography from the SRT was used together with the MIP to create the final map. The results (Figure 14) show that the bedrock slopes downwards towards NNW, and this, together with the NW groundwater flow, can explain the extension of the plume.

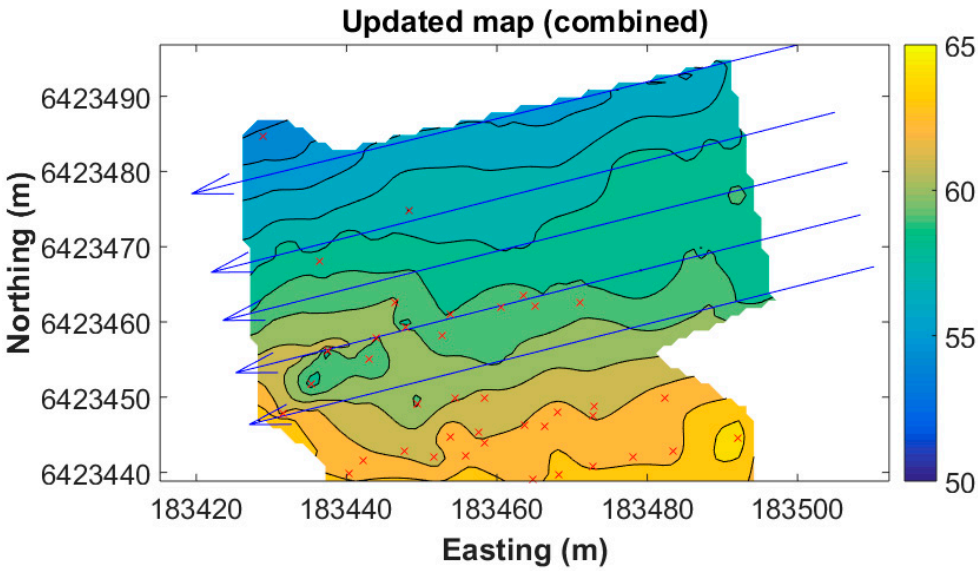

Figure 14. Final bedrock topography estimated by combining the results from the MIP and SRT methods.

Last, the DCIP monitoring system data collected before the bioremediation was initiated, has been used to map the geology in the area. The results are in good correlation with the geological profiles (Figure 13), although the lithology seems more heterogeneous than was previously thought. Furthermore, there is a strong increase in the electrical resistivity observed in Line 3 and Line 4 that can be correlated with high concentrations of contaminants in those areas (Figure 15). The correlation between the geoelectrical measurements and the contaminants, as well as the heterogeneity of the soil, is evident in the inverted result of the cross-hole tomography (Figure 16).

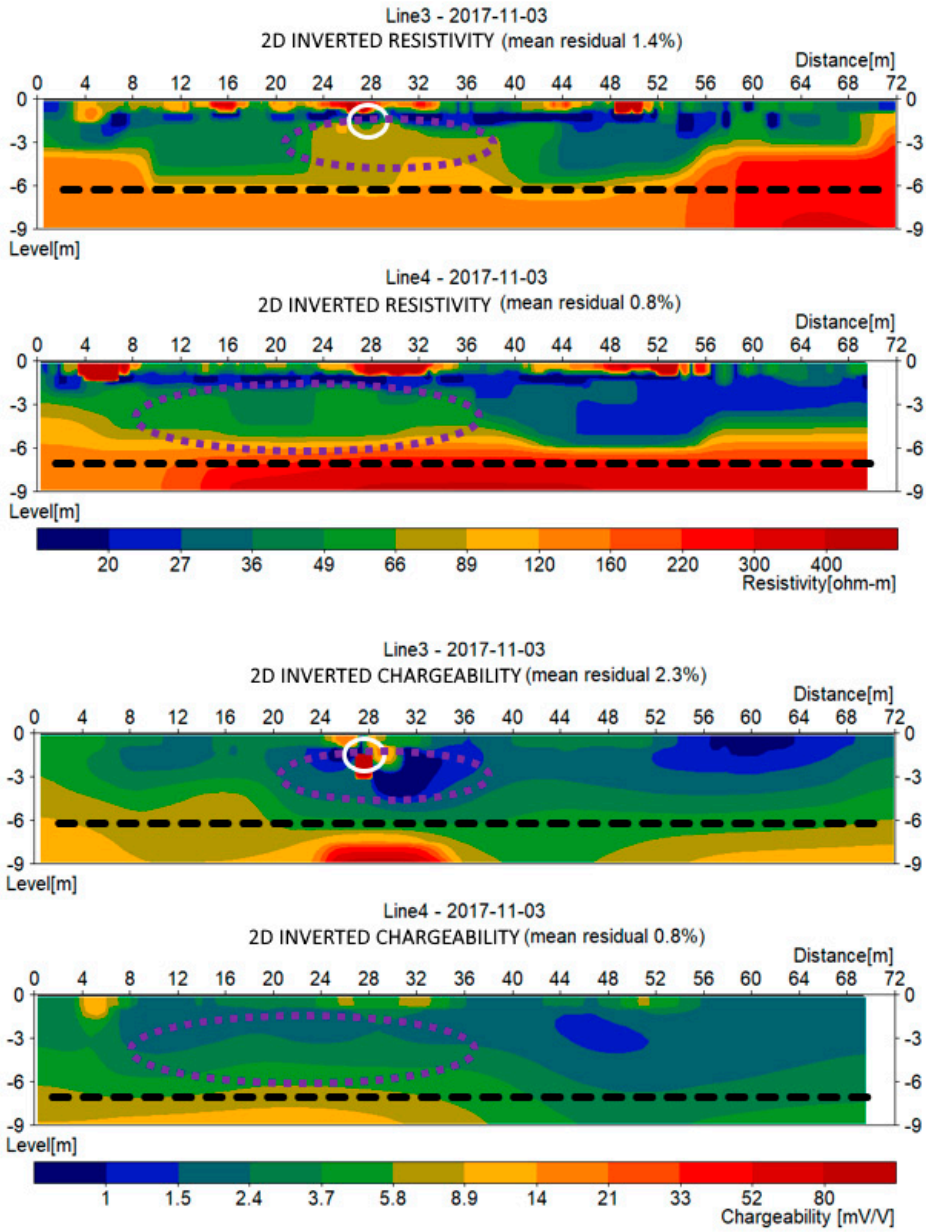

Figure 15. DCIP results from the baseline survey, November 2017 showing the interpreted bedrock (black dashed line), the interpreted contamination (purple dashed circle) and the location of buried metal infrastructure (white circle)

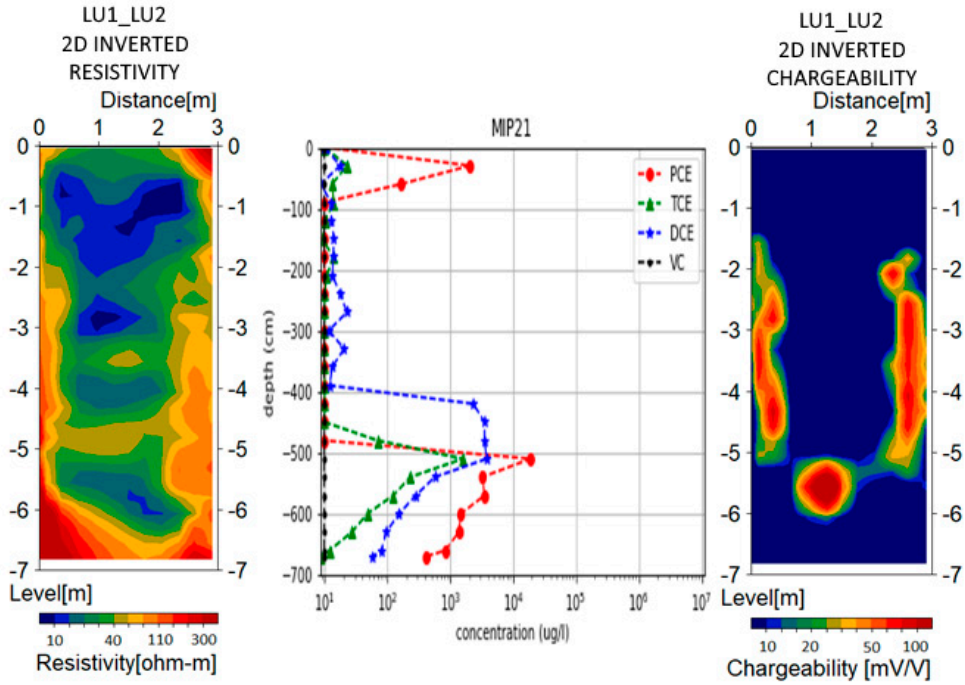

Figure 16. Inverted cross-hole tomography results for LU1-LU2. Resistivity (left), chargeability (right) and concentration from MIP sounding (middle).

Paper II

A robust scheme for pre-processing, inversion and visualization of monitoring data is presented. 20-months of daily data were used in this work.

First, the time-series data from individual quadrupoles where filtered using first a median filter and then a low pass Butterworth filter to remove outliers. The proposed approach is very fast and can be used to effectively remove outliers from the data before the inversion.

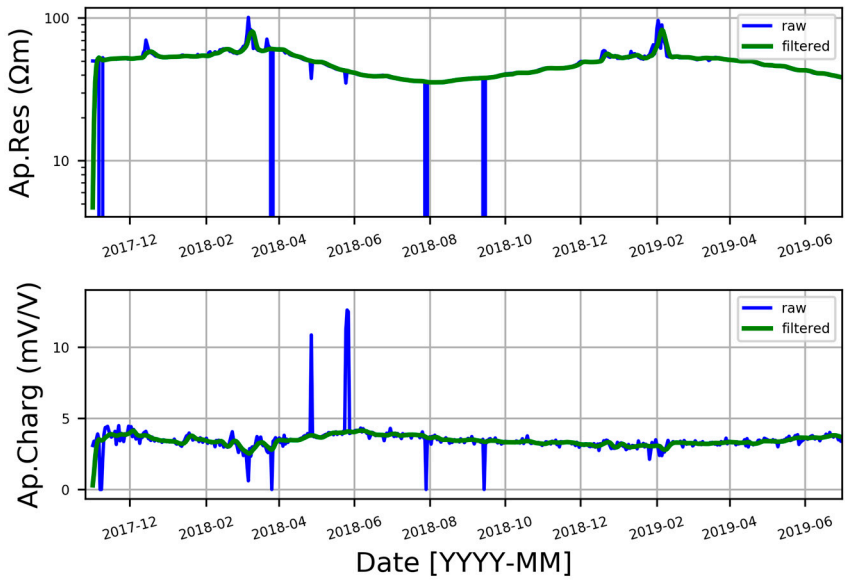

Figure 17. Example of filtering of raw data for quadrupole 34 of Line 3. The example refers to the data point involving electrodes distance 7-16-13-14 meters (A-B-M-N).

The data were inverted using the time-lapse algorithm. First, using the data from the baseline a reference profile was calculated and then weekly (median) profiles were computed for the entire dataset (20 months). The weekly profiles were finally inverted against the reference baseline profile.

The inverted results (Figure 18) show that the two treated areas behave differently during the 20-month period after the remediation program was launched. The area treated with the iron particles (Line 3) shows a general decrease in the electrical resistivity that dominates the entire time period. On the other hand, the area treated with the mixture of bacteria (Line 3) appears more resistive as the time progress.

Figure 19 illustrate the change in resistivity and chargeability for three areas of interest, the two treated areas and a reference area that no treatment took place. A block of 10x2 meter was selected for each area and the average value for the % change in resistivity and the change in chargeability is presented. It is evident that the resistivity values in the area where they injected the iron particles (Figure 19b, east area) are reduced significantly when compared with the baseline. On the other hand, the area where they injected the bacteria (Figure 19a, west area) and the untreated area (Figure 19c, end of Line 3) appear to change in a very similar way. That could mean that either the method fails to identify changes due to the effects of remediation or the experiment was unsuccessful.

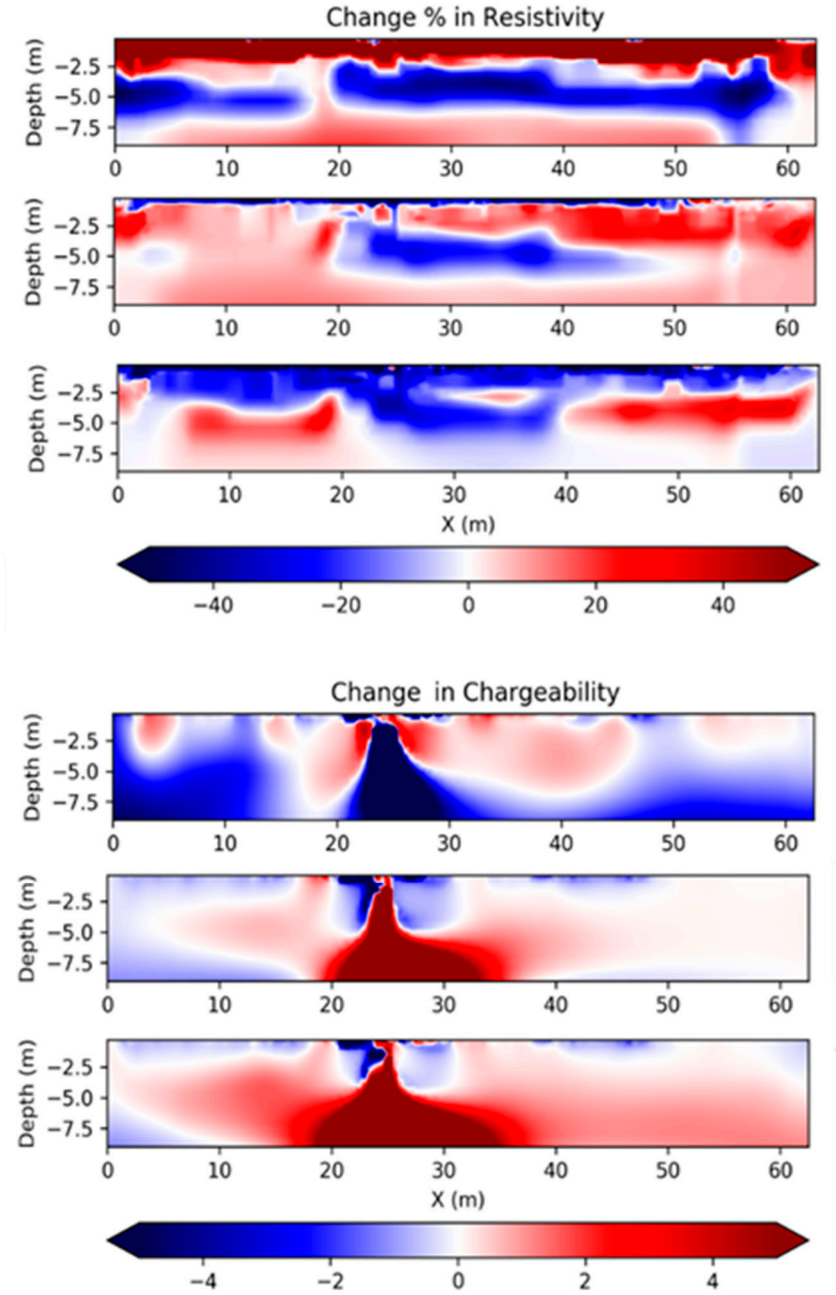

Figure 18. Examples of time-lapse inversions of Line3: from dates 2018-03-08 (top row), 2018-10-21 (middle row) and 2019-02-27 (bottom row). Percentage change in resistivity (top three) and absolut change in chargeability (bottom three) compared to baseline dataset.

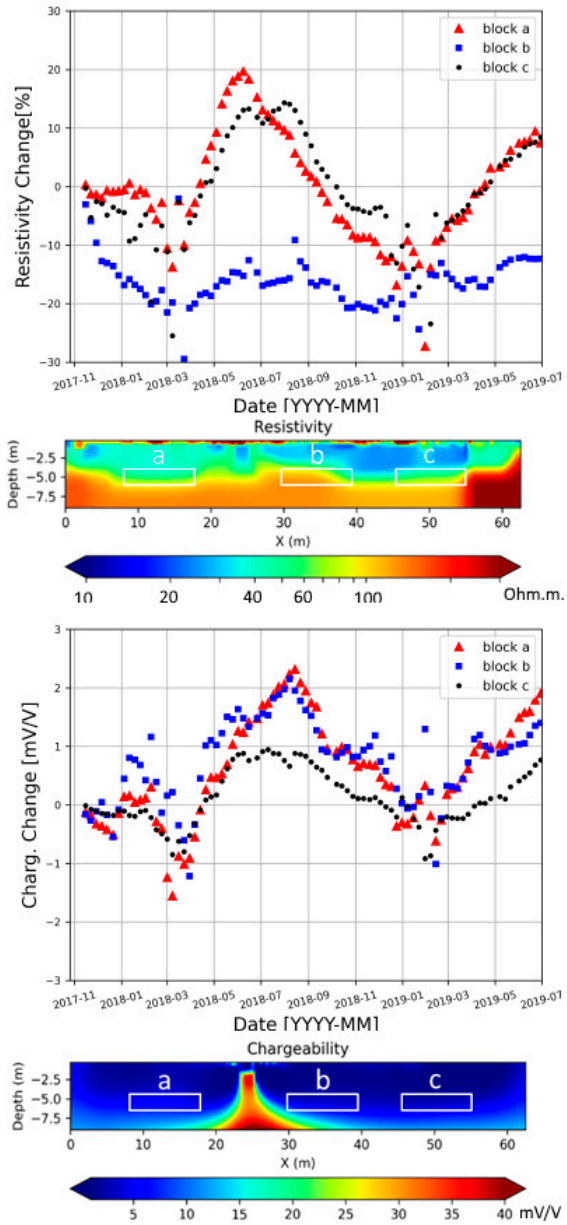

Figure 19. Analysis of the time dependent variations of resistivity (top) and chargeability (bottom) for Line 3. Resistivity is represented as percentage changes of inverted data respect to background, while chargeability is the absolute variation of inverted integral chargeability respect to background values. The values of the plots are calculated averaging inside the three areas (a, b, c) highlighted in the inverted results from the baseline below the respective time dependent variations.

Chapter 6. Conclusions and future work

The work presented in this thesis demonstrates the effectiveness of geophysical methods for site characterization and mapping of the contamination. The use of point specific information, such as drillings or wells, is very important to make an accurate interpretation of the geophysical data. Furthermore, the geophysical data can be used to extrapolate the point specific information and create models that have greater spatial coverage.

The DCIP method has several advantages in monitoring of in-situ bioremediation. A permanent installation of the system along with several automation routines in terms of data acquisition and pre-processing, significantly reduces the cost of geophysical site investigation. The proposed data workflow can establish a robust framework that may be used as a base for a fully autonomous system, that could generate a result as soon as a new time step is recorded, bringing geoelectrical monitoring one step closer to real-time monitoring.

Future work

The inverted profiles are strongly affected by seasonal variations due to temperature among other factors, so the inverted results need to be corrected for the temperature. Removing the effect of the temperature from the inverted profiles will highlight the changes that take place due to the injection of the products and the bioremediation.

Information from hydrogeochemical sampling should be used to verify the geophysical results, especially the results from Paper II. It is a relevant fact that the geoelectrical signature of the treated area (west) follows the same pattern as the untreated area which may mean that the treatment applied in the western treated area is not effective in reducing contamination as desired.

The spectral information contained in the DCIP data was not used in this work. It remains a challenge to propose robust routines that can be universally applied to large datasets, which would remove outliers and prepare the data for the inversion.

The use of neural networks could possibly be a solution to that problem. The spectral content can be further analysed for variations in time due to the remediation.

Hydrogeological models can be used to estimate the flow of the fluids in the subsurface. The hydrogeological models can be used to understand how the subsurface behaves and what to expect in the future. The geoelectrical monitoring can be used for example, to calibrate the hydrogeological models. Hydrogeophysics for in-situ bioremediation is indeed a very challenging field that can provide valuable tools for planning and monitoring of a bioremediation plan.

Chapter 7. References

Abdulsamad, F., Revil, A., Soueid Ahmed, A., Coperey, A., Karaoulis, M., Nicaise, S., Peyras, L., 2019. Induced polarization tomography applied to the detection and the monitoring of leaks in embankments. Engineering Geology 254, 89–101. https://doi.org/10.1016/j.enggeo.2019.04.001

Angelis, D., Tsourlos, P., Tsokas, G., Vargemezis, G., Zacharopoulou, G., Power, C., 2018. Combined application of GPR and ERT for the assessment of a wall structure at the Heptapyrgion fortress (Thessaloniki, Greece). Journal of Applied Geophysics 152, 208–220. https://doi.org/10.1016/j.jappgeo.2018.04.003

Argote-Espino, D.L., López-García, P.A., Tejero-Andrade, A., 2016. 3D-ERT geophysical prospecting for the investigation of two terraces of an archaeological site northeast of Tlaxcala state, Mexico. Journal of Archaeological Science: Reports 8, 406–415. https://doi.org/10.1016/j.jasrep.2016.06.047

Atekwana, E.A., Atekwana, E., Legall, F.D., Krishnamurthy, R.V., 2005. Biodegradation and mineral weathering controls on bulk electrical conductivity in a shallow hydrocarbon contaminated aquifer. Journal of Contaminant Hydrology 80, 149–167. https://doi.org/10.1016/j.jconhyd.2005.06.009

Atekwana, E.A., Atekwana, E.A., 2010. Geophysical signatures of microbial activity at hydrocarbon contaminated sites: A review. Surveys in Geophysics 31, 247–283. https://doi.org/10.1007/s10712-009-9089-8

Auken, E., Doetsch, J., Fiandaca, G., Christiansen, A.V., Gazoty, A., Cahill, A.G., Jakobsen, R., 2014. Imaging subsurface migration of dissolved CO2 in a shallow aquifer using 3-D time-lapse electrical resistivity tomography. Journal of Applied Geophysics 101, 31–41. https://doi.org/10.1016/j.jappgeo.2013.11.011

Bernstone, C., Dahlin, T., Ohlsson, T., Hogland, W., 2000. DC-resistivity mapping of internal landfill structures: Two pre-excavation surveys. Environmental Geology 39, 360–371. https://doi.org/10.1007/s002540050015

Branzen, H., 2013. Förstärkt självrening av grundvatten förorenat med klokerade etener.

Cassiani, G., Kemna, A., Villa, A., Zimmermann, E., 2009. Spectral induced polarization for the characterization of free-phase hydrocarbon contamination of sediments with low clay content. Near Surface Geophysics 7, 547–562.

Caterina, D., Flores Orozco, A., Nguyen, F., 2017. Long-term ERT monitoring of biogeochemical changes of an aged hydrocarbon contamination. Journal of Contaminant Hydrology 201, 19–29. https://doi.org/10.1016/j.jconhyd.2017.04.003

Chambers, J.E., Kuras, O., Meldrum, P.I., Ogilvy, R.D., Hollands, J., 2006. Electrical resistivity tomography applied to geologic, hydrogeologic, and engineering investigations at a former waste-disposal site. GEOPHYSICS 71, B231–B239. https://doi.org/10.1190/1.2360184

Chambers, J.E., Meldrum, P.I., Gunn, D.A., Wilkinson, P.B., Kuras, O., Weller, A.L., Ogilvy, R.D., 2009. Hydrogeophysical monitoring of landslide processes using automated time-lapse electrical resistivity tomography (ALERT). Presented at the Near Surface 2009 - 15th European Meeting of Environmental and Engineering Geophysics. https://doi.org/10.3997/2214-4609.20147066

Chirindja, F.J., Dahlin, T., Juizo, D., 2017. Improving the groundwater-well siting approach in consolidated rock in Nampula Province, Mozambique. Hydrogeology Journal 25, 1423–1435. https://doi.org/10.1007/s10040-017-1540-1

Cook, K.L., Van Nostrand, R.G., 1954. Interpretation of Resistivity Data Over Filled Sinks. Geophysics 19, 761–790.

Dahlin, T., Loke, M.H., 2015. Negative apparent chargeability in time-domain induced polarisation data. Journal of Applied Geophysics 123, 322–332. https://doi.org/10.1016/j.jappgeo.2015.08.012

Dahlin, T., Zhou, B., 2006. Multiple-gradient array measurements for multichannel 2D resistivity imaging. Near Surface Geophysics 4, 113–123.

Danielsen, B.E., Dahlin, T., 2009. Comparison of geoelectrical imaging and tunnel documentation at the Hallandsås Tunnel, Sweden. Engineering Geology 107, 118–129. https://doi.org/10.1016/j.enggeo.2009.05.005

Davis, C.A., Atekwana, E., 2006. Potential application of biogeophysics to EOR and remediation investigations. SEG Technical Program Expanded Abstracts 25, 1471–1474. https://doi.org/10.1190/1.2369798

Fernandez, P.M., Bloem, E., Binley, A., Philippe, R.S.B.A., French, H.K., 2019. Monitoring redox sensitive conditions at the groundwater interface using electrical resistivity and self-potential. Journal of Contaminant Hydrology 226. https://doi.org/10.1016/j.jconhyd.2019.103517

Fetter, C.W., 2001. Applied Hydrogeology, 4th ed. Prentice Hall.

Flores Orozco, A., Velimirovic, M., Tosco, T., Kemna, A., Sapion, H., Klaas, N., Sethi, R., Bastiaens, L., 2015. Monitoring the injection of microscale zerovalent iron particles for groundwater remediation by means of complex electrical conductivity imaging. Environmental Science and Technology 49, 5593–5600. https://doi.org/10.1021/acs.est.5b00208

Flores Orozco, A., Williams, K.H., Kemna, A., 2013. Time-lapse spectral induced polarization imaging of stimulated uranium bioremediation. Near Surface Geophysics 11, 531–544. https://doi.org/10.3997/1873-0604.2013020

Forquet, N., French, H.K., 2012. Application of 2D surface ERT to on-site wastewater treatment survey. Journal of Applied Geophysics 80, 144–150. https://doi.org/10.1016/j.jappgeo.2012.02.002

Gazoty, A., Fiandaca, G., Pedersen, J., Auken, E., Christiansen, A., Pedersen, J., 2012a. Application of time domain induced polarization to the mapping of lithotypes in a landfill site. Hydrology and Earth System Sciences 16, 1793–1804. https://doi.org/10.5194/hess-16-1793-2012

Gazoty, A., Fiandaca, G., Pedersen, J., Auken, E., Christiansen, A.V., 2012b. Mapping of landfills using time-domain spectral induced polarization data: the Eskelund case study. Near Surface Geophysics 10, 575–586. https://doi.org/10.3997/1873-0604.2012046

Giang, N.V., Kochanek, K., Vu, N.T., Duan, N.B., 2018. Landfill leachate assessment by hydrological and geophysical data: case study NamSon, Hanoi, Vietnam. Journal of Material Cycles and Waste Management 20, 1648–1662. https://doi.org/10.1007/s10163-018-0732-7

Johansson, S., Sparrenbom, C., Fiandaca, G., Lindskog, A., Olsson, P.-I., Dahlin, T., Rosqvist, H., 2017. Investigations of a Cretaceous limestone with spectral induced polarization and scanning electron microscopy. Geophysical Journal International 208, 954–972. https://doi.org/10.1093/gji/ggw432

Kemna, A., Binley, A., Slater, L., 2004. Crosshole IP imaging for engineering and environmental applications. Geophysics 69, 97–107. https://doi.org/10.1190/1.1649379

Kim, J.-H., Supper, R., Tsourlos, P.I., Yi, M.-J., 2013. 4D Inversion of Resistivity Monitoring Data through Lp Norm Minimizations. Geophysical Journal International 195, 1640–1656. https://doi.org/10.1093/gji/ggt324

Knödel, K., Lange, G., Voigt, H.-J., 2007. Environmental Geology: Handbook of Field Methods and Case Studies. Springer-Verlag, Berlin Heidelberg. https://doi.org/10.1007/978-3-540-74671-3

Kuras, O., Wilkinson, P.B., Meldrum, P.I., Oxby, L.S., Uhlemann, S., Chambers, J.E., Binley, A., Graham, J., Smith, N.T., Atherton, N., 2016. Geoelectrical monitoring of simulated subsurface leakage to support high-hazard nuclear decommissioning at the Sellafield Site, UK. Science of The Total Environment 566–567, 350–359. https://doi.org/10.1016/j.scitotenv.2016.04.212

Leroux, V., Dahlin, T., 2006. Time-lapse resistivity investigations for imaging saltwater transport in glaciofluvial deposits. Environmental Geology 49, 347–358. https://doi.org/10.1007/s00254-005-0070-7

Leroux, V., Dahlin, T., Rosqvist, H., 2010. Time-domain IP and resistivity sections measured at four landfills with different contents. Presented at the Near Surface 2010 - 16th European Meeting of Environmental and Engineering Geophysics. https://doi.org/10.3997/2214-4609.20144851

Loke, M., Barker, R.D., 1996. Rapid Least-Squares Inversion of Apparent Resistivity Pseudosections Using a Quasi-Newton Method. Geophysical Prospecting 44, 131–152. https://doi.org/10.1111/j.1365-2478.1996.tb00142.x

Loke, M.H., Chambers, J.E., Rucker, D.F., Kuras, O., Wilkinson, P.B., 2013. Recent developments in the direct-current geoelectrical imaging method. Journal of Applied Geophysics 95, 135–156. https://doi.org/10.1016/j.jappgeo.2013.02.017

Loke, M.H., Dahlin, T., Leroux, V., 2011. Constrained time-lapse inversion of 3-D resistivity surveys data. Presented at the Near Surface 2011 - 17th European Meeting of Environmental and Engineering Geophysics.

Loke, M.H., Dahlin, T., Rucker, D.F., 2014. Smoothness-constrained time-lapse inversion of data from 3D resistivity surveys. Near Surface Geophysics 12, 5–24. https://doi.org/10.3997/1873-0604.2013025

Maurya, P.K., Balbarini, N., Møller, I., Rønde, V., Christiansen, A.V., Bjerg, P.L., Auken, E., Fiandaca, G., 2018. Subsurface imaging of water electrical conductivity, hydraulic permeability and lithology at contaminated sites by induced polarization. Geophysical Journal International 213, 770–785. https://doi.org/10.1093/gji/ggy018

Ntarlagiannis, D., Robinson, J., Soupios, P., Slater, L., 2016. Field-scale electrical geophysics over an olive oil mill waste deposition site: Evaluating the information content of resistivity versus induced polarization (IP) images for delineating the spatial extent of organic contamination. Journal of Applied Geophysics 135, 418–426. https://doi.org/10.1016/j.jappgeo.2016.01.017

Olsson, P.-I., Dahlin, T., Fiandaca, G., Auken, E., 2015. Measuring time-domain spectral induced polarization in the on-time: Decreasing acquisition time and increasing signal-to-noise ratio. Journal of Applied Geophysics 123, 316–321. https://doi.org/10.1016/j.jappgeo.2015.08.009

Olsson, P.-I., Fiandaca, G., Larsen, J.J., Dahlin, T., Auken, E., 2016. Doubling the spectrum of time-domain induced polarization by harmonic de-noising, drift correction, spike removal, tapered gating and data uncertainty estimation. Geophysical Journal International 207, 774–784. https://doi.org/10.1093/gji/ggw260

Park, S., Yi, M.-J., Kim, J.-H., Shin, S.W., 2016. Electrical resistivity imaging (ERI) monitoring for groundwater contamination in an uncontrolled landfill, South Korea. Journal of Applied Geophysics, New trends in Induced Polarization 135, 1–7. https://doi.org/10.1016/j.jappgeo.2016.07.004

Power, C., Gerhard, J.I., Karaoulis, M., Tsourlos, P., Giannopoulos, A., 2014. Evaluating four-dimensional time-lapse electrical resistivity tomography for monitoring DNAPL source zone remediation. Journal of Contaminant Hydrology 162–163, 27–46. https://doi.org/10.1016/j.jconhyd.2014.04.004

Power, C., Tsourlos, P., Ramasamy, M., Nivorlis, A., Mkandawire, M., 2018. Combined DC resistivity and induced polarization (DC-IP) for mapping the internal composition of a mine waste rock pile in Nova Scotia, Canada. Journal of Applied Geophysics 150, 40–51. https://doi.org/10.1016/j.jappgeo.2018.01.009

Rosqvist, H., Leroux, V., Dahlin, T., Svensson, M., Lindsjö, M., Månsson, C.-H., Johansson, S., 2011. Mapping landfill gas migration using resistivity monitoring. Proceedings of the Institution of Civil Engineers - Waste and Resource Management 164, 3–15. https://doi.org/10.1680/warm.2011.164.1.3

Rossi, M., Dahlin, T., Olsson, P.-I., Günther, T., 2018. Data acquisition, processing and filtering for reliable 3D resistivity and time-domain induced polarisation tomography in an urban area: Field example of Vinsta, Stockholm. Near Surface Geophysics 16, 220–229. https://doi.org/10.3997/1873-0604.2018014

SEPA, 2014. Nationell Plan för Fördelning av Statliga Bidrag för Efterbehandling; Report 6617. Swedish Environmental Protection Agency: Stockholm, Sweden Volume 30.

Simyrdanis, K., Moffat, I., Papadopoulos, N., Kowlessar, J., Bailey, M., 2018a. 3D Mapping of the Submerged Crowie Barge Using Electrical Resistivity Tomography. International Journal of Geophysics 2018. https://doi.org/10.1155/2018/6480565

Simyrdanis, K., Papadopoulos, N., Soupios, P., Kirkou, S., Tsourlos, P., 2018b. Characterization and monitoring of subsurface contamination from Olive Oil Mills' waste waters using Electrical Resistivity Tomography. Science of the Total Environment 637–638, 991–1003. https://doi.org/10.1016/j.scitotenv.2018.04.348

Slater, L., Ntarlagiannis, D., Yee, N., O'Brien, M., Zhang, C., Williams, K.H., 2008. Electrodic voltages in the presence of dissolved sulfide: Implications for monitoring natural microbial activity. Geophysics 73, F65–F70. https://doi.org/10.1190/1.2828977

Slater, L.D., Lesmes, D., 2002. IP interpretation in environmental investigations. Geophysics 67, 77–88. https://doi.org/10.1190/1.1451353

Sparrenbom, C.J., Åkesson, S., Johansson, S., Hagerberg, D., Dahlin, T., 2017. Investigation of chlorinated solvent pollution with resistivity and induced polarization. Science of The Total Environment 575, 767–778. https://doi.org/10.1016/j.scitotenv.2016.09.117

Steelman, C.M., Klazinga, D.R., Cahill, A.G., Endres, A.L., Parker, B.L., 2017. Monitoring the evolution and migration of a methane gas plume in an unconfined sandy aquifer using time-lapse GPR and ERT. Journal of Contaminant Hydrology 205, 12–24. https://doi.org/10.1016/j.jconhyd.2017.08.011

Tsourlos, P.I., Ogilvy, R.D., 1999. An algorithm for the 3-D inversion of tomographic resistivity and induced polarisation data: Preliminary results. Journal of the Balkan Geophysical Society 2, 30–45.

Ustra, A.T., Elis, V.R., Mondelli, G., Zuquette, L.V., Giacheti, H.L., 2012. Case study: A 3D resistivity and induced polarization imaging from downstream a waste disposal site in Brazil. Environmental Earth Sciences 66, 763–772. https://doi.org/10.1007/s12665-011-1284-5

Wemegah, D.D., Fiandaca, G., Auken, E., Menyeh, A., Danuor, S.K., 2017. Spectral time-domain induced polarisation and magnetic surveying - An efficient tool for characterisation of solid waste deposits in developing countries. Near Surface Geophysics 15, 75–84. https://doi.org/10.3997/1873-0604.2016048

White, D.J., 1989. Two-Dimensional Seismic Refraction Tomography. Geophys J Int 97, 223–245. https://doi.org/10.1111/j.1365-246X.1989.tb00498.x

Zago, M.M., Fries, M., Ramires, J.E.F., 2020. Groundwater infiltration in a gold mine–A geoelectrical investigation model as an aid to dewatering process determination. Journal of Applied Geophysics 172. https://doi.org/10.1016/j.jappgeo.2019.103909